Generalized Frequency Division Multiplexing with Index Modulation

Ersin Öztürk[1,2], Ertugrul Basar[1], Hakan Ali Çırpan[1]
[1]Istanbul Technical University, Faculty of Electrical and Electronics Engineering, 34469, Maslak, Istanbul, Turkey
Email: ersinozturk, basarer, cirpanh@itu.edu.tr
[2]Netas, Department of Research and Development, 34912, Pendik, Istanbul, Turkey
Email: eozturk@netas.com.tr

***Abstract*—Generalized frequency division multiplexing (GFDM) is a promising non-orthogonal multicarrier transmission scheme which has recently received a great deal of attention towards future fifth generation (5G) wireless networks. It overcomes the limitations of orthogonal frequency division multiplexing (OFDM) while preserving most of the advantages of it. On the other hand, index modulation (IM) has the potential to provide a flexible system design with adjustable number of active subcarriers as well as significant bit error rate (BER) performance improvement for multicarrier systems. In this paper, we propose the combined application of GFDM and IM techniques. We present the GFDM-IM system model and evaluate its error performance by comparing to classical GFDM and OFDM-IM for Rayleigh multipath fading channels. It is shown via computer simulations that the GFDM-IM system achieves signicantly better error performance than classical GFDM due to the information bits carried in the spatial domain by the indices of active GFDM subcarriers.**

I. Introduction

Owing to its attractive properties, orthogonal frequency division multiplexing (OFDM) has been the most common multicarrier transmission scheme for current broadband wireless communication systems and it fulfills the requirements and challenges of fourth generation (4G) networks. On the other hand, the scenarios foreseen for future fifth generation (5G) wireless networks have requirements such as very high spectral efficiency, relaxed synchronization, very low latency and low out-of-band (OOB) emission [1]. Although OFDM provides some attractive advantages such as robustness to frequency selective fading and easy implementation, it falls short to address the requirements of 5G networks satisfactorily. As a result, alternative multicarrier transmission schemes are currently being evaluated as potential candidates for 5G wireless networks such as filter bank multicarrier (FBMC) [2], universal filtered multicarrier (UFMC) [3] and generalized frequency division multiplexing (GFDM) [4].

GFDM is a generalized form of OFDM [5] in which a GFDM symbol has a block structure consisting of KM samples where K subcarriers carry M timeslots each. Therefore, a GFDM symbol includes a group of OFDM symbols. Since GFDM uses only one cyclic prefix (CP) per symbol, spectral efficiency of GFDM is higher than that of OFDM. On the other hand, the insertion of CP enables low-complexity frequency domain equalization (FDE). In GFDM, circular pulse shaping is applied for each subcarrier. This reduces OOB emission significantly; as a result, GFDM can serve for fragmented and opportunistic spectrum allocation purposes. Since it is a non-orthogonal multicarrier scheme, GFDM can tolerate loose time and frequency synchronization. Furthermore, block structure of GFDM permits flexible time and frequency partitioning. Therefore, it is possible to reduce the latency on the physical layer (PHY) of communications systems. Consequently, GFDM appears as a potential scheme to fulfill the requirements and challenges of 5G wireless networks.

There is a continuous effort to provide better spectral efficiency in order to increase data transmission rate. Spatial modulation (SM) is a novel multiple input multiple output (MIMO) transmission technique which uses the spatial domain to convey information in addition to the classical Q-ary signal constellations. SM employs active transmit antenna indices to carry additional information bits [6]. For SM multicarrier schemes, only one transmit antenna is activated by the input bit sequences at any subcarrier [7]. SM is an extension of two dimensional signal constellations to a new third dimension, which is the spatial (antenna) dimension. Inspired by the pioneering idea of SM, OFDM with index modulation (OFDM-IM) is a recently proposed novel scheme which transmits information not only by constellation symbols, but also by the indices of the active subcarriers that are activated according to the corresponding information bits [8]–[10].

IM concept for OFDM has attracted significant attention during recent times due to its appealing advantages over classical OFDM such as flexible system design with adjustable number of active subcarriers and improved error performance for low-to-mid spectral efficiencies [11]. It has been recently proved in [12] that the combination of OFDM-IM and MIMO transmission techniques provides an interesting trade-off among error performance, spectral efficiency and decoding complexity. Furthermore, it has been demonstrated in [13] that OFDM-IM also provides improvements over classical OFDM in terms of ergodic achievable rate. However, the combination of GFDM with IM remains an open as well as interesting research problem.

In this paper, considering the potential of IM for classical

978-1-5090-2482-7/16/$31.00 ©2016 IEEE

OFDM, we investigate the combination of the IM technique with GFDM. The main contributions of this paper are the construction of the GFDM-IM system model and the evaluation of its bit error ratio (BER) performance for Rayleigh multipath fading channels. It is shown via computer simulations that the GFDM-IM system achieves signicantly better error performance than classical GFDM due to the employment of IM for GFDM subcarriers.

The remaining sections are organized as follows. Section II describes the basic principles of GFDM. In Section III, we present the GFDM-IM system model. Section IV evaluates the BER performance of the GFDM-IM system with respect to the classical GFDM and OFDM-IM systems for Rayleigh multipath fading channels. Finally, Section V concludes the paper.

II. GFDM BACKGROUND

GFDM has a block structure consisting of K subcarriers with M timeslots on each of it. The total number of samples in a GFDM block is given as $N = KM$. The baseband model of the overall GFDM transmit signal $x(n)$ of one block is given by

$$x(n) = \sum_{k=0}^{K-1} \sum_{m=0}^{M-1} d_{k,m} g_{k,m}(n), \qquad n = 0, \ldots, N-1 \quad (1)$$

where n denotes the sampling index, $d_{k,m}$ denotes the complex valued data symbol, which is taken from a Q-QAM (Q-ary quadrature amplitude modulation) constellation, of the kth subcarrier and mth timeslot, and

$$g_{k,m} = g\left((n - mK)_{\text{mod}N}\right) \exp\left(j2\pi \frac{kn}{K}\right) \quad (2)$$

is the transmit filter circularly shifted to the mth timeslot and modulated to the kth subcarrier. After collecting the filter samples in a vector $g_{k,m} = [g_{k,m}(0), \ldots, g_{k,m}(N-1)]^T$, (1) can be rewritten as

$$\mathbf{x} = \mathbf{A}\mathbf{d} \quad (3)$$

where $\mathbf{d}$ is a $KM \times 1$ column vector containing $d_{k,m}$ as its $(mK+k)$th element and $\mathbf{A}$ is a $KM \times KM$ transmitter matrix [5] with the following structure:

$$\mathbf{A} = [\mathbf{g}_{0,0}, \ldots, \mathbf{g}_{K-1,0}, \mathbf{g}_{0,1}, \ldots, \mathbf{g}_{K-1,1}, \ldots, \mathbf{g}_{K-1,M-1}]. \quad (4)$$

The last step at the transmitter side is the addition of a CP with length N_{CP} in order to avoid intersymbol interference (ISI).

At the receiver side, the first stage is the removal of CP. We assume that the length of the channel impulse response is shorter than the CP and transmitter and receiver are perfectly synchronized. Under these assumptions, the received signal after the removal of CP can be written as

$$\mathbf{y} = \mathbf{H}\mathbf{x} + \mathbf{w} = \mathbf{H}\mathbf{A}\mathbf{d} + \mathbf{w} \quad (5)$$

where $\mathbf{H}$ is an $N \times N$ circular convolution matrix constructed from the channel impulse response, $\mathbf{w}$ is the vector of additive white Gaussian noise (AWGN) samples with elements having zero mean and σ_w^2 variance. After zero-forcing (ZF) channel equalization,

$$\mathbf{z} = \mathbf{H}^{-1}\mathbf{H}\mathbf{A}\mathbf{d} + \mathbf{H}^{-1}\mathbf{w} = \mathbf{A}\mathbf{d} + \overline{\mathbf{w}} \quad (6)$$

is obtained and linear demodulation of the signal can be expressed as

$$\hat{\mathbf{d}} = \mathbf{B}\mathbf{z} \quad (7)$$

where $\mathbf{B}$ is the $KM \times KM$ receiver matrix. Different linear detection approaches can be used to recover the transmitted symbols. Two commonly used data detection approaches, namely the matched filter receiver $\mathbf{B}_{\text{MF}} = \mathbf{A}^H$ and ZF receiver $\mathbf{B}_{\text{ZF}} = \mathbf{A}^{-1}$ can be applied in (7) to recover the data vector $\mathbf{d}$. Additionally, minimum mean square error (MMSE) approach can be directly used in (5) to joint equalization and detection (JED) by using $\mathbf{B}_{\text{MMSE}} = \left(\mathbf{R}_w + \mathbf{A}^H\mathbf{H}^H\mathbf{H}\mathbf{A}\right)^{-1}\mathbf{A}^H\mathbf{H}^H$ where $\mathbf{R}_w$ denotes the covariance matrix of the noise vector. Note that for the case of JED, the ZF channel equalizer block is not required and $\hat{\mathbf{d}} = \mathbf{B}_{\text{MMSE}}\mathbf{y}$.

III. GFDM-IM SYSTEM MODEL

As mentioned earlier, GFDM has a block structure consisting of KM samples where K subcarriers constitute a GFDM subsymbol and M GFDM subsymbols constitute a GFDM symbol. CP-OFDM is a special case of GFDM where M is equal to one. In this context, GFDM-IM system model can be constructed as a generalization of the OFDM-IM system model given in [8]. In contrast to OFDM-IM, GFDM-IM subcarriers can be non-orthogonal to each other due to non-rectangular pulse shaping. While the introduction of non-orthogonal subcarriers increases the flexibility of the scheme and allows the control of various properties of the signal, negative effects such as self-created intercarrier interference (ICI) and ISI that degrades the BER performance occur. ICI can be mitigated by employing interference cancellation techniques and ISI are avoided by the appropriate choice of the pulse shape [14]. However, non-rectangular pulse shaping prohibits straightforward subcarrier decomposition. Block diagram of the proposed GFDM-IM system is shown in Fig. 1.

A. GFDM-IM Transmitter

As shown in Fig. 1, primary bit splitter takes L information bits as input and divides these L bits into M groups each containing l bits, i.e., $l = L/M$. Then, secondary bit splitter divides these l bits into q groups each containing p bits, i.e., $p = l/q$. Additionally, the subcarriers of each GFDM subsymbol are divided into q groups each containing n_q subcarriers, where $n_q = K/q$. Therefore, total number of subcarrier groups in a GFDM symbol becomes $N_q = Mq$. Then, each group of p bits is mapped to a subcarrier group of length n_q. This mapping operation both use ordinary Q-QAM constellations and indices of the active subcarriers. For each subcarrier group, only k_q out of n_q available subcarriers are selected as active and modulated. These subcarriers are determined by the first p_1 bits of incoming p-bit sequence by

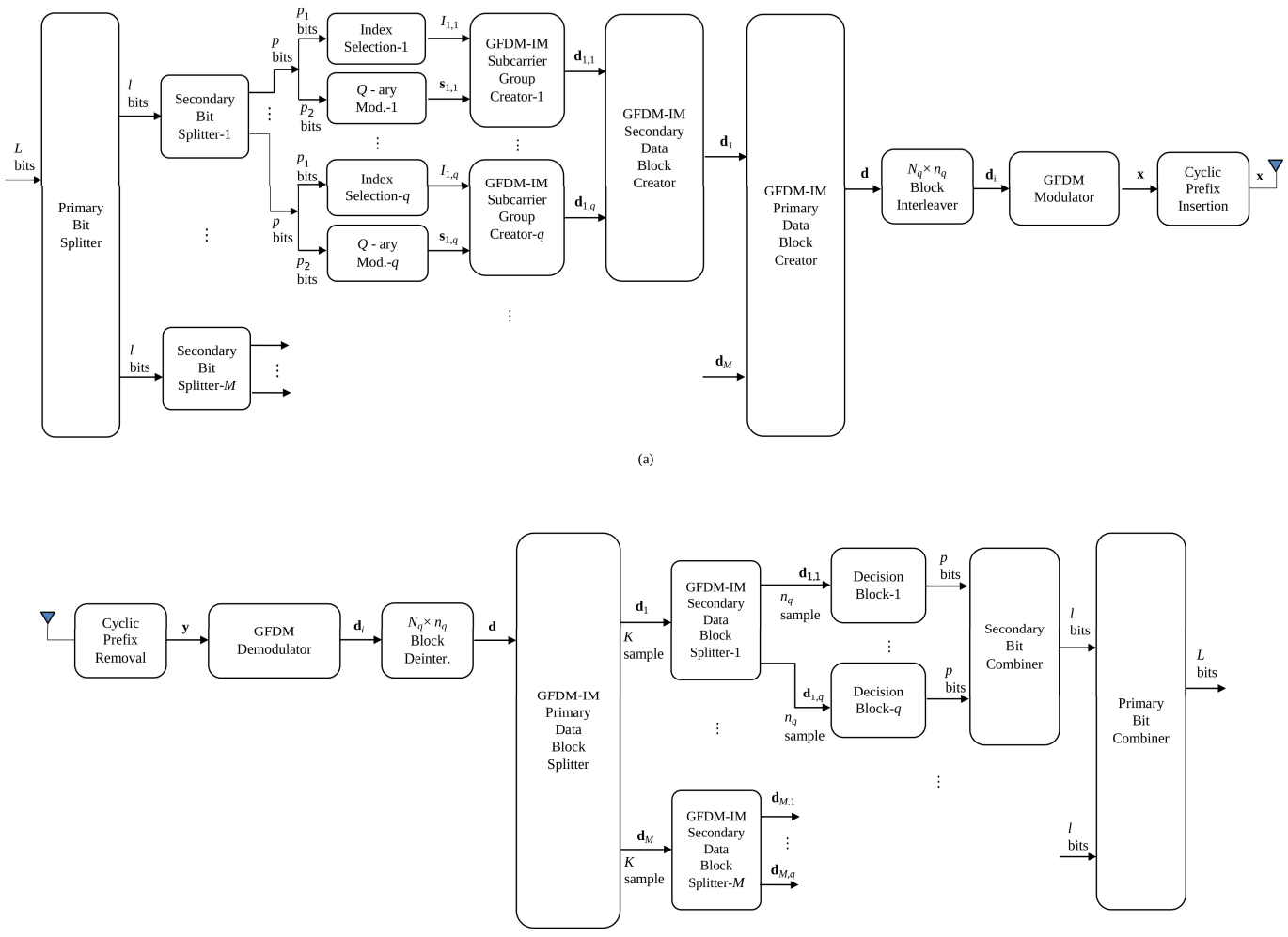

Fig. 1. GFDM-IM system model, (a) GFDM-IM transmitter, (b) GFDM-IM receiver.

a selection rule, and the selected subcarrier indices are given by

$$I_{m,\beta} = \left\{ i_{m,\beta,1}, i_{m,\beta,2}, \ldots, i_{m,\beta,k_q} \right\} \tag{8}$$

where $i_{m,\beta,\gamma} \in [1, \ldots, n_q]$, for $m = 1, \ldots, M$, $\beta = 1, \ldots, q$ and $\gamma = 1, \ldots, k_q$. Since $I_{m,\beta}$ has $c = 2^{p_1}$ possible realizations, only c out of $C\left(n_q, k_q\right)$ possible combinations are used. Therefore, p_1 can be defined as

$$p_1 = \lfloor \log_2 \left(C\left(n_q, k_q\right) \right) \rfloor. \tag{9}$$

The remaining bits of p-bit sequence are mapped to the Q-ary signal constellation. Since k_q out of n_q available subcarrier are selected as active, we obtain

$$p_2 = k_q \log_2 Q. \tag{10}$$

In other words, p_2 bits are used to determine the data symbols that modulate the subcarriers having active indices. As a result, the vector of the modulated symbols for a subcarrier group, which carries p_2 bits, can be expressed by

$$\mathbf{s}_{m,\beta} = \left[s_{m,\beta}\left(1\right), s_{m,\beta}\left(2\right), \ldots, s_{m,\beta}\left(k_q\right) \right]^T \tag{11}$$

where $s_{m,\beta}\left(\gamma\right) \in \mathcal{S}$, for $m = 1, \ldots, M$, $\beta = 1, \ldots, q$, $\gamma = 1, \ldots, k_q$. Then, GFDM-IM subcarrier group creator sets inactive subcarriers to zero and the resulting vector of transmit symbols for a subcarrier group (m, β) is given by

$$\mathbf{d}_{m,\beta} = \left[d_{m,\beta}\left(1\right), d_{m,\beta}\left(2\right), \ldots, d_{m,\beta}\left(n_q\right) \right]^T \tag{12}$$

where $d_{m,\beta}\left(\nu\right) \in \{0, \mathcal{S}\}$, for $m = 1, \ldots, M$, $\beta = 1, \ldots, q$ and $\nu = 1, \ldots, n_q$. After that, GFDM-IM secondary data block creator combines the transmit symbol vectors $\mathbf{d}_{m,\beta}$ and forms the data block for subsymbol m as

$$\mathbf{d}_m = \left[{\mathbf{d}_{m,1}}^T, {\mathbf{d}_{m,2}}^T, \ldots, {\mathbf{d}_{m,q}}^T \right]^T. \tag{13}$$

Finally, GFDM-IM primary data block creator combines the data blocks $\mathbf{d}_m$ and forms the main data block for a GFDM symbol as

$$\mathbf{d} = \left[{\mathbf{d}_1}^T, {\mathbf{d}_2}^T, \ldots, {\mathbf{d}_q}^T \right]^T. \tag{14}$$

which contains $N = KM$ elements. However, opposite to classical GFDM, $\mathbf{d}$ contains some zero terms whose positions carry additional information bits for GFDM-IM. In [12], [15], [16], in order to ensure that the subcarriers of a subcarrier

group are affected by uncorrelated wireless fading channels, a block interleaver is considered after the formation of the main data block. Therefore, an $N_q \times n_q$ block interleaver is applied to $\mathbf{d}$ and the interleaved data vector $\mathbf{d}_i$ is obtained.

After block interleaving, GFDM data block $\mathbf{d}_i$ is modulated using a GFDM modulator according to system model in (3) and the vector $\mathbf{x}$, which contains transmit samples for a GFDM symbol, is obtained. A CP with length N_{CP} is appended to the beginning of $\mathbf{x}$ and the resulting vector

$$\tilde{\mathbf{x}} = \left[\mathbf{x}\left(KM - N_{\text{CP}} + 1 : KM\right)^T, \mathbf{x}^T\right]^T \tag{15}$$

is obtained. Finally, $\tilde{\mathbf{x}}$ is transmitted over a frequency-selective Rayleigh fading channel which is described by $\mathbf{H}$ and corrupted by AWGN samples with variance σ_w^2. $\mathbf{H}$ is an $N \times N$ circular convolution matrix constructed from the channel impulse response coefficients

$$\mathbf{h} = [h_1, h_2, \ldots, h_{N_{\text{ch}}}]^T \tag{16}$$

where h_τ, $\tau = 1, 2, \ldots, N_{\text{ch}}$ are circularly symmetric complex Gaussian random variables with variance $1/N_{\text{ch}}$.

B. GFDM-IM Receiver

At the receiver side, the first stage is the removal of CP. After CP removal, under the assumption that CP is longer than N_{ch} and perfect synchronization is ensured, the received signal $\mathbf{y}$ can be expressed as in (5).

The second stage of the receiver is GFDM demodulation. As mentioned earlier, there are three different approaches to recover the transmitted symbols. The MF receiver maximizes the signal-to-noise (SNR) ratio while introducing self-interference. The ZF receiver removes self-interference; however, it enhances noise. The MMSE receiver balances self-interference and noise and performs the best among these three methods. In this study, MMSE estimation is used and the linear demodulation of the received signal can be expressed as

$$\hat{\mathbf{d}}_i = \mathbf{B}_{\text{MMSE}}\mathbf{y}. \tag{17}$$

After GFDM demodulation, $N_q \times n_q$ block deinterleaving is performed and the estimation of the GFDM-IM primary data block creator output vector $\hat{\mathbf{d}}$ is obtained. Then, GFDM-IM primary data block splitter divides this data block $\hat{\mathbf{d}}$ into M groups each containing K samples and the estimation of the GFDM-IM secondary data block creator output vector $\hat{\mathbf{d}}_m$ is obtained. After that, GFDM-IM secondary data block splitter divides these K samples into q groups each containing n_q samples and the estimation of the GFDM-IM subcarrier group creator output vector $\hat{\mathbf{d}}_{m,q}$ is obtained. Then, decision block processes the estimated data block $\hat{\mathbf{d}}_{m,q}$ and tries to determine the active subcarriers and detect their corresponding information symbols. At this stage, decision block calculates the Euclidean distances between the estimated data block $\hat{\mathbf{d}}_{m,q}$ and all possible subcarrier index combinations as well as signal constellation points (i.e., over all possible subcarrier block realizations) and makes a joint decision on the active indices and the constellation symbols by minimizing the following metric:

$$\tilde{\mathbf{d}}_{m,\beta} = \underset{\mathbf{d}_{m,\beta}}{\operatorname{argmin}} \left\|\hat{\mathbf{d}}_{m,\beta} - \mathbf{d}_{m,\beta}\right\|_F^2 \tag{18}$$

Decision block obtains the active indices $\hat{I}_{m,\beta}$ and the constellation symbols $\tilde{\mathbf{s}}_{m,\beta}$ from $\tilde{\mathbf{d}}_{m,\beta}$ and recovers the information bits by applying the inverse mapping process for both modulated symbols and indices of the active subcarriers. Then, secondary bit combiner combines the outputs of the decision blocks and forms the l-bit sequence which is the estimate of the input of secondary bit splitter. Finally, primary bit combiner combines all the l-bit groups and forms the L information bits.

C. Computational Complexity

GFDM-IM transmitter differs from classical GFDM transmitter by the employment of IM and block interleaving. Since we do not perform any multiplication operation for the IM and block interleaving, the computational complexity of the GFDM-IM transmitter and classical GFDM transmitter is assumed to be identical. In addition, since $N_q \times n_q$ block interleaving is applied in GFDM symbol boundary, it does not insert any latency. On the other hand, GFDM-IM receiver differs from classical GFDM receiver by the block deinterleaver and decision metrics for the transmitted data symbols and active subcarrier positions. Searching for all possible subcarrier index combinations and signal constellation points in the decision block causes additional Euclidean distance calculations which increase the computational complexity of the receiver. As in the transmitter, block deinterleaving does not affect the computational complexity and the latency. One GFDM data block includes KM QAM symbols. There are Q elements in symbol constellation. Therefore, the decision block of classical GFDM receiver performs KMQ Euclidean distance calculations to determine the closest constellation points for the GFDM data block. On the other hand, there are N_q subcarrier groups in one GFDM-IM data block and $c = 2^{p_1}$ possible subcarrier index combinations in one subcarrier group. Since there are k_q subcarriers in one subcarrier index combination, Q^{k_q} QAM symbol combinations exist for one subcarrier index combination. As a result, the decision block of GFDM-IM receiver performs$N_q k_q c Q^{k_q}$ Euclidean distance calculations to determine the closest constellation points for the GFDM-IM data block. Consequently, the computational complexity of GFDM-IM receiver increases by $Q^{k_q - 1}$ with the increasing values of Q. The complexity of the formation of $\mathbf{B}_{\text{MMSE}}$ is the same for GFDM and GFDM-IM schemes.

D. Spectral Efficiency

According to [8], the spectral efficiency of the OFDM-IM scheme can be given by

$$\eta_{\text{OFDM-IM}} = \frac{\frac{K}{n_q}\left(\left\lfloor \log_2\left(C\left(n_q, k_q\right)\right)\right\rfloor + k_q \log_2 Q\right)}{K + N_{\text{CP}}} \tag{19}$$

TABLE I
SIMULATION PARAMETERS

Description	Parameter	Value
Number of subcarriers	K	128
Number of subsymbols	M	5
GFDM demodulator	$\mathbf{B}$	MMSE
Pulse shaping filter	g	RRC
Length of cyclic prefix	N_{CP}	32
Exponent of power delay profile	ϕ	0.1
Number of channel taps	N_{TAP}	10

TABLE II
A LOOK-UP TABLE EXAMPLE FOR $n = 4, k = 2$ AND $p_1 = 2$

Bits	*Indices*	*subblocks*
[0 0]	$\{1, 2\}$	$[s_\chi \; s_\zeta \; 0 \; 0]^T$
[0 1]	$\{2, 3\}$	$[0 \; s_\chi \; s_\zeta \; 0]^T$
[1 0]	$\{3, 4\}$	$[0 \; 0 \; s_\chi \; s_\zeta]^T$
[1 1]	$\{1, 4\}$	$[s_\chi \; 0 \; 0 \; s_\zeta]^T$

For the GFDM-IM system, spectral efficiency becomes

$$\eta_{\text{GFDM-IM}} = \frac{M\frac{K}{n_q}\left(\lfloor \log_2\left(C\left(n_q, k_q\right)\right)\rfloor + k_q \log_2 Q\right)}{MK + N_{\text{CP}}} \tag{20}$$

On the other hand, the spectral efficiency of the GFDM scheme is given by

$$\eta_{\text{GFDM}} = \frac{MK \log_2 Q}{MK + N_{\text{CP}}} \tag{21}$$

Using (19), (20) and (21), the spectral efficiency gain of the GFDM-IM system over OFDM-IM becomes

$$\rho = \frac{1 + \frac{N_{\text{CP}}}{K}}{1 + \frac{N_{\text{CP}}}{MK}} \tag{22}$$

and the spectral efficiency gain of the GFDM-IM system over GFDM system becomes

$$\rho' = \frac{k_q}{n_q} + \frac{\lfloor \log_2\left(C\left(n_q, k_q\right)\right)\rfloor}{n_q \log_2 Q} \tag{23}$$

As seen from (23), the spectral efficiency gain of the GFDM-IM system over the GFDM system is dependent on k_q, n_q and Q. In some cases, by properly choosing k_q and n_q, the spectral efficiency of the GFDM-IM scheme can exceed that of classical GFDM without increasing the size of the signal constellation.

IV. RESULTS AND DISCUSSION

In this section, the BER performance of the proposed GFDM-IM system has been compared with classical GFDM and OFDM-IM systems for Rayleigh multipath fading channels. System parameters used in computer simulations are presented in Table I. MMSE receiver is used as the GFDM demodulator and the chosen pulse shape for the GFDM prototype filter is the root-raised cosine (RRC) filter. In order to investigate the effect of the pulse shape on the GFDM-IM system, roll-off factor (a) of 0.1 and 0.9 are used. We assume that the transmitter and the receiver are perfectly synchronized and the receiver has perfect channel state information. In

TABLE III
A LOOK-UP TABLE EXAMPLE FOR $n = 4, k = 3$ AND $p_1 = 2$

Bits	*Indices*	*subblocks*
[0 0]	$\{1, 2, 3\}$	$[s_\chi \; s_\zeta \; s_\delta \; 0]^T$
[0 1]	$\{1, 2, 4\}$	$[s_\chi \; s_\zeta \; 0 \; s_\delta]^T$
[1 0]	$\{1, 3, 4\}$	$[s_\chi \; 0 \; s_\zeta \; s_\delta]^T$
[1 1]	$\{2, 3, 4\}$	$[0 \; s_\chi \; s_\zeta \; s_\delta]^T$

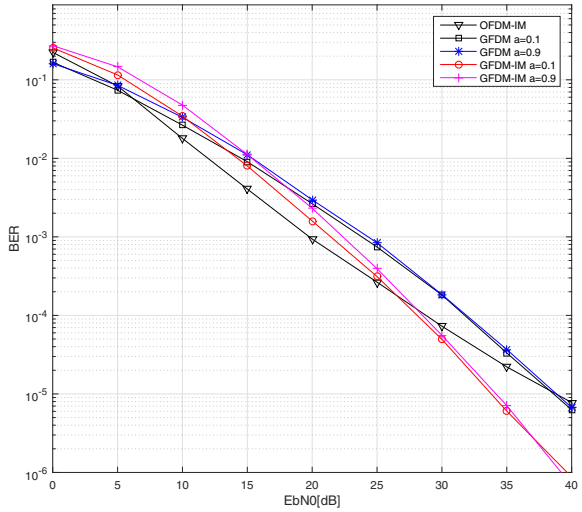

Fig. 2. BER performance of GFDM, GFDM-IM and OFDM-IM for BPSK transmission with roll-off factor (a) of 0.1 and 0.9 and look-up table given in Table II.

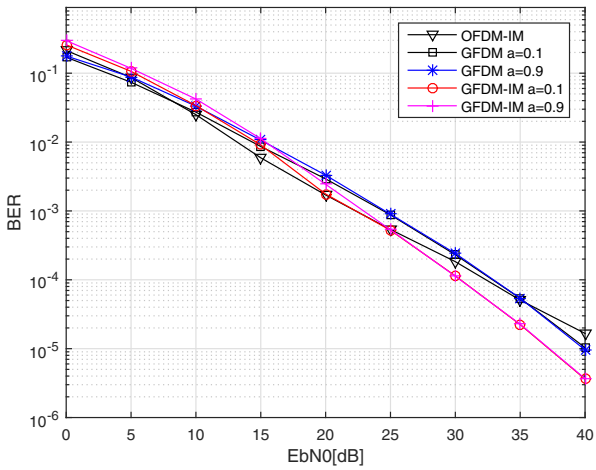

Fig. 3. BER performance of GFDM, GFDM-IM and OFDM-IM for 4-QAM transmission with roll-off factor (a) of 0.1 and 0.9 and look-up table given in Table III.

order to determine the active subcarrier indices, look-up table method is used. Two look-up tables, which are presented in Tables II and III, are created.

Fig. 2 shows the BER performance of the GFDM, the GFDM-IM and the OFDM-IM systems for binary phase shift keying (BPSK) transmission in Rayleigh multipath channel using the look-up table given in Table II. From Fig. 2, it is observed that the error performance of the GFDM-IM system becomes slightly worse than the GFDM system below 15 dB as in the OFDM-IM system in [8]. For high SNR values, the GFDM-IM system provides approximately 5 dB better BER performance than the classical GFDM system for a target BER value of 10^{-5} at the same spectral efficiency. The reason behind this BER performance improvement of the GFDM-IM scheme can be explained by the improved Euclidean distance spectrum due to IM. On the other hand, at a BER value of 10^{-5}, the GFDM-IM system achieves approximately 5 dB better BER performance than the OFDM-IM system. This improvement in BER performance can be explained by inherently existing frequency diversity in GFDM due to transmitting one subsymbol on several frequency samples. It is observed that increasing the roll-off factor slightly degrades the performance. It is possible to conclude that BER performance improvement of the GFDM-IM system with respect to the classical GFDM system is quite similar to the BER performance improvement of the OFDM-IM system in [8] with respect to the classical OFDM system.

Fig. 3 shows the BER performance of the GFDM, the GFDM-IM and the OFDM-IM systems for 4-QAM transmission in Rayleigh multipath channel using the look-up table given in Table III. From Fig. 3, it is observed that the error performance of the GFDM-IM and the GFDM systems are nearly identical for low SNR values. For high SNR values, the GFDM-IM system provides approximately 3 dB better BER performance than both the classical GFDM system and the OFDM-IM system as in BPSK transmission case.

As mentioned earlier, transmitter complexity of the GFDM system and the GFDM-IM system is identical. Therefore, this significant BER improvement of the proposed GFDM-IM system is provided without increasing the transmitter complexity. As a result, by using GFDM-IM scheme, it is possible to reduce the transmit power of a mobile terminal in an uplink scenario. On the other hand, for the configuration given in Tables I and II, while decision block of the GFDM receiver performs 1280 complex multiplications per one GFDM symbol, the decision block of the GFDM-IM receiver performs 5120 complex multiplications per one GFDM symbol for BPSK transmission. As a result, the proposed GFDM-IM receiver requires four times higher complex multiplications. On the other hand, the complexity increase at the receiver is not a major concern for an uplink scenario where the base station has relaxed power and space constraints with respect to the mobile terminal. However, GFDM-IM system can provide an interesting trade-off between complexity and BER performance for downlink transmission scenarios. Furthermore, spectral efficiency gain of the GFDM-IM system over OFDM-IM system for the configurations given in Tables I, II and III is 19%.

V. CONCLUSION

In this paper, a novel multicarrier modulation scheme, which is constructed by the combination of GFDM and IM, has been proposed. The system model of the proposed GFDM-IM system has been presented and its BER performance has been compared to classical GFDM system under Rayleigh multipath fading channels. It has been demonstrated that the proposed GDFM-IM system provides significant BER improvement compared to classical GFDM system without increasing the transmitter complexity. As a result, by using GFDM-IM scheme, it is possible to reduce the transmit power of a mobile terminal in an uplink scenario. We conclude that GFDM-IM scheme can be considered a promising candidate for future 5G wireless networks.

REFERENCES

[1] G. Wunder *et. al.*, "5GNOW: Non-orthogonal, asynchronous waveforms for future mobile applications," *IEEE Commun. Mag.*, vol. 52, no. 2, pp. 97–105, Feb. 2014.

[2] B. Farhang-Boroujeny, "OFDM versus filter bank multicarrier," *IEEE Signal Process. Mag.*, vol. 28, no. 3, pp. 92–112, May 2011.

[3] V. Vakilian, T. Wild, F. Schaich, S. ten Brink, and J. F. Frigon, "Universal filtered multi-carrier technique for wireless systems beyond LTE," in *IEEE Globecom Workshop*, Atlanta, GA, USA, Dec. 2013, pp. 223–228.

[4] G. Fettweis, M. Krondorf, and S. Bittner, "GFDM - Generalized Frequency Division Multiplexing," in *69th IEEE VTC Spring*, Barcelona, Spain, Apr. 2009, pp. 1–4.

[5] N. Michailow, M. Matth, I. Gaspar, A. Caldevilla, L. Mendes, A. Festag, and G. Fettweis, "Generalized frequency division multiplexing for 5th generation cellular networks," *IEEE Trans. Commun.*, vol. 62, no. 9, pp. 3045–3061, Sep. 2014.

[6] R. Mesleh, H. Haas, C. W. Ahn, and S. Yun, "Spatial modulation-a new low complexity spectral efficiency enhancing technique," in *CHINACOM*, Oct. 2006, pp. 1–5.

[7] R. Mesleh, H. Haas, C. W. Sinanovic, C. W. Ahn, and S. Yun, "Spatial modulation," *IEEE Trans. Veh. Technol.*, vol. 57, no. 4, pp. 2228–2241, Jul. 2008.

[8] E. Basar, Ü. Aygölü, E. Panayırcı, and H. V. Poor, "Orthogonal frequency division multiplexing with index modulation," *IEEE Trans. Signal Process.*, vol. 61, no. 22, p. 55365549, Nov. 2013.

[9] R. Abu-alhiga and H. Haas, "Subcarrier-index modulation OFDM," in *IEEE Int. Sym. Personal, Indoor and Mobile Radio Commun.*, Tokyo, Japan, Sep. 2009, p. 177181.

[10] D. Tsonev, S. Sinanovic, and H. Haas, "Enhanced subcarrier index modulation (SIM) OFDM," in *IEEE GLOBECOM Workshops*, Dec. 2011, p. 728732.

[11] E. Basar, "Index modulation techniques for 5G wireless networks," *IEEE Commun. Mag.*, vol. 54, no. 7, pp. 168–175, Jul. 2016.

[12] ——, "On multiple-input multiple-output OFDM with index modulation for next generation wireless networks," *IEEE Trans. Signal Process.*, vol. 64, no. 15, pp. 3868–3878, Aug. 2016.

[13] M. Wen, X. Cheng, M. Ma, B. Jiao, and H. V. Poor, "On the achievable rate of OFDM with index modulation," *IEEE Trans. Signal Process.*, vol. 64, no. 8, pp. 1919–1932, Apr. 2016.

[14] B. M. Alves, L. L. Mendes, D. A. Guimaraes, and I. S. Gaspar, "Performance of GFDM over frequency-selective channels," in *Int. Workshop on Telecommun.*, Santa Rita do Sapuca, Brazil, May 2013.

[15] X. Cheng *et. al.*, "Index modulated OFDM with interleaved grouping for V2X communications," in *IEEE Int. Conf. Intell. Transport. Syst. (ITSC)*, Qingdao, China, Oct. 2014.

[16] Y. Xiao *et. al.*, "OFDM with interleaved subcarrier-index modulation," *IEEE Commun. Lett.*, vol. 18, no. 8, pp. 1447–1450, Jun. 2014.